ISSN: 2573-962X

Research article

Journal of Pharmaceutical Research

Dry Powder Inhalation Formulation of PLGA/PEG microparticles: Optimization of Spray Drying with the Box-Behnken Design

Srushti J. Sodha* and Pardeep K. Gupta

Department of Pharmaceutical Sciences, St. Joseph's University, 600 S 43rd Street, Philadelphia, PA, 19104

***Corresponding Author**
Srushti J. Sodha. Address: St. Joseph's University, 600 S 43rd Street, Philadelphia, PA, 19104.

Submitted: 2023, Sep 12; **Accepted:** 2023, Oct 02; **Published:** 2023, Oct 10

Citation: Sodha, S. J., Gupta, P. K. (2023). Dry Powder Inhalation Formulation of PLGA/PEG microparticles: Optimization of Spray Drying with the Box-Behnken Design. *J Pharmaceut Res, 8*(2), 262-270.

Abstract

Large, porous microparticles have emerged as an attractive platform for pulmonary delivery of therapeutic proteins. While the large size and porosity imparts buoyancy and lung dispersibility, tailoring the polymer surface characteristics enables retention of protein stability and desirable release profile. Previously, we developed porous PLGA microparticles with PLGA 50501A and established stability and controlled release of Somatropin for 7 days. PEG was established as a multifunctional pore former – providing benefits of polymer plasticization, improved drug loading and stability. The goal of the current study is scaling up the system to obtain a robust, platform process for large scale manufacturing of porous PLGA/PEG microparticles with diameters between 5 – 12 µm, low densities (<0.4 g/cm3), high porosity using Buchi mini-spray dryer. Design of Experiments using Box-Behnken design was used to develop and validate a mathematical model correlating microparticle characteristics to the operation parameters.

Keywords: Spray Drying, Porous PLGA Microparticles, Pulmonary Protein Delivery, Box-Behnken Design.

1. Introduction

Large, porous MPs with diameters between 5 – 12 µm and low densities (<0.4 g/cm3) are emerging as suitable platforms for pulmonary protein delivery due to their buoyancy, lung dispersibility and ability to evade pulmonary macrophage clearance [01, 02]. Spray Drying is a simple, rapid, robust, and continuous process. It is an attractive approach for development of polymeric micro and nano-carriers due to its compatibility with various liquid feeds to yield dry powders and scalability [03, 04]. Besides, it exhibits a multitude of advantages such as low operating costs and high energy efficient [03, 04]. Several studies have used spray drying for preparation of low density MPs without the incorporation of any pore forming agent [05]. Introduction of porosity by incorporation of salts (NaCl) and effervescent agents is also prevalent. However, the incorporation of most inorganic compounds requires emulsification of the feed to form single or double emulsions [02, 06-08]. Introduction of porosity using novel techniques such as ultrasound and piezoelectric spray drying have also been evaluated [09, 04]. However, preparation of a homogeneous feed solution with both polymer and pore former incorporated in the organic phase is relatively rare, and usually is observed with lyophilic pore-formers which require washing with organic solvents such as hexane for leaching [07].

Our process aims to bridge these gaps by exhibiting the following advantages.

1. The feed is a homogeneous solution with PLGA (polymer), and polyethylene glycol (PEG) dissolved in tetrahydrofuran. Circumventing the emulsification step not only reduces a couple of unit operations, but also eliminates the variability arising due to globule size distribution and emulsion stability.
2. PEG is a highly hydrophilic pore-former, thereby eliminates the need for leaching with an organic solvent. This a therefore a green process.
3. Aside from imparting porosity, PEG is known to be multifunctional [05, 10–14]. It plasticizes PLGA by relieving the polymer chain tension and thereby increasing the surface charge density, which enhances drug loading (discussed subsequently) [13]. It is also shown to prevent burst release and enhance biocompatibility of polymeric formulations [05].

Somatropin, also known as recombinant human growth hormone (r-hGH), is the only available as subcutaneous injections for chronic replacement therapy in growth hormone deficiency (GHD). GHD can be juvenile, idiopathic or acquired by trauma to the pituitary gland, and is characterized by short stature, poor organ and tissue development and regeneration and/or mental retardation [15]. r-hGH has a serum half-life of 19 – 35 minutes. Previously, we developed porous PLGA 50501A microparticles with diameters between 5 – 12µm and low densities (<0.4 g/cm^3) and loaded r-HGH by adsorption. The Drug loading was characterized at pH 4.0 (acidic), 5.3 (pI) and pH 7.2 (neutral) and was a result of an interplay of electrostatic and hydrophobic

interactions between the polymer and somatropin. Considering the physicochemical interactions, we observed some pH dependent protein unfolding characterized by reduction in intrinsic fluorescence of the Tryptophan 86 residue at 331 nm. The secondary α-helix structure characterized by 2 negative minima at 209 nm and 222 nm in the circular dichroism spectra, was intact at all pH values. R-hGH was released over a period of seven days, and the release profile was a function of the microparticle porosity.

Design of Experiments (DoE) was implemented for optimization of the spray drying process. This approach not only allows establishment of correlations between the input and output parameters, but also helps development of a mathematical model for the same. It allows the users a flexibility to optimize the process with minimum experiments, to quantify and understand the interactions between the factors, visualize the variation in responses as a function of factors and choose the optimal value of responses to derive an operation space/ point.

We prepared a dry powder for inhalation (DPI) comprising of spray dried, porous PLGA MPs. These had diameters ranging from 5 – 23 µm, aerodynamic diameters of 2 – 9 µm, densities of 0.1 to 0.3 g/cc. True densities were measured with helium gas adsorption, and porosities computed using geometric diameters and density ranged from 70 – 80%.

2. Materials

Recombinant human growth hormone (r-hGH) was obtained from Bresagen, Inc. (Adelaide, Australia) in the form of a lyophilized powder and was used as is. PLGA 5050 1A was obtained from Evonik Corporation (Parsippany, NJ). Polyethylene glycol (PEG 3350) was obtained from Spectrum pharmacy products. Nanopure water used to make buffer solutions and to reconstitute lyophilized protein was purified by reverse osmosis (Barnstead Ultra filtered type I water). All buffer components (2-(N-morpholino) ethane sulfonic acid (MES), sodium chloride, sodium hydroxide and hydrochloric acid) were of analytical grade and purchased from Sigma-Aldrich (St. Louis, MO). Other experimental materials were acquired from Fisher Scientific Co. (Fairlawn, NJ).

3. Methods

3.1. Spray Drying to prepare porous PLGA MPs:

PLGA 5050 1A (molecular weight 10kDa, uncapped, lactic: glycolic ratio 1:1) was previously established to provide maximum stability for r-hGH[16]. PLGA and PEG 3350 in ratio 100:15 was dissolved in dichloromethane (for preliminary studies) and tetrahydrofuran (for optimization studies) at different total solid concentrations as stated in table 1 to form a homogeneous solution. Spray drying was carried out using a Buchi 190-Mini Spray Dryer (Buchi, Flawil, Switzerland). The operating conditions were as follows: nozzle diameter 0.5 mm, air flow rate (table 1), sample pumping speed 8.5 mL/min, 100% aspiration, inlet temperature (table 1). The spray dried particles were then stirred in nanopure water for 2 hours to leach the pore former (PEG). The particles were then filtered and lyophilized to obtain dry powders.

Std	Run	Temperature (oC)	Feed concentration (% w/v)	Air flow rate (mm Hg)	Diameter (µm)	Yield (%)	True density (g/cm^3)	Bulk Density (g/cm^3)	Porosity (%)	MMAD (µm)
8	1	60	10	40	6.1	73.9	0.92	0.27	70.9	2.7
10	2	50	15	25	21.5	51.6	0.93	0.20	78.8	8.2
7	3	40	10	40	7.25	43.8	0.90	0.22	75.7	2.9
13	4	50	10	32.5	15.1	62.1	0.92	0.22	75.8	6.1
5	5	40	10	25	17.3	34.6	0.92	0.21	77.7	6.8
12	6	50	15	40	17.1	59	0.90	0.24	73.5	7.2
6	7	60	10	25	17.1	70.4	0.92	0.23	75.2	7.1
4	8	60	15	32.5	16.8	72.1	0.95	0.23	75.6	7.0
1	9	40	5	32.5	13.2	47.7	0.91	0.25	73.0	5.6
9	10	50	5	25	6.5	54.3	0.92	0.26	71.4	2.9
11	11	50	5	40	5.9	66.8	0.92	0.22	76.1	2.4
2	12	60	5	32.5	5.9	77.1	0.92	0.21	77.2	2.3
3	13	40	15	32.5	22.2	38.4	0.93	0.20	78.7	8.6

Table 1. Design of experiments runs, and characterization of large, porous PLGA/PEG MPs prepared by spray drying.

3.2. Optimization of spray drying process parameters using Design of Experiments (DoE)

The experimental design and data analysis for optimizing the process parameters for spray dried porous PLGA MPs was conducted using Design Expert ® software, version 10 (Stat-Ease, Inc, Minneapolis, USA). Temperature (oC), feed concentration (% w/v) and air flow rate (mmHg) were regarded as crucial parameters. Based on the number of factors and their levels, Box-Behnken design was employed, using multiple regression statistics. A linear model was fitted to the corrected responses. P values for each factor were used to determine their significance for spray drying of porous MPs. The responses were set considering the size distribution of the obtained MPs and to maximize the percentage yield.

The effect of independent variables [Temperature (oC) - A, feed concentration (% w/v) - B and air flow rate (mmHg) - C] on dependent variables [particle size (µm) - R1, and percentage yield (%) - R2] was studied as shown in table 1.

The Stat-Ease software designed 13 experimental runs, as mentioned in table 1. ANOVA was performed to evaluate factor coefficients and the significance of the model. To validate the model and to check its reproducibility, batches predicted by software were performed and analyzed.

3.3. Characterization of porous MPs:

The porous MPs prepared by spray drying were characterized for percentage yield, geometrical and aerodynamic diameters as well as bulk and true densities.

The percentage yield of porous MPs was calculated by measuring the number of MPs obtained (yactual, grams) to the theoretical number of MPs (Ytheo, grams) using equations 1 and 2.

$$\% \text{ Yield} = (Y_{actual} / Y_{theo}) \text{ X } 100 \ldots\ldots\ldots\ldots\ldots \quad \text{Equation 1}$$

Y_{theo} = (Concentration of feed sprayed) X (Volume of feed sprayed) …… Equation 2

The particles were characterized for particle size using laser diffraction. The particles were dispersed in purified water, the dispersion was sonicated and added to the hydrocyte chamber of the Mastersizer 3000 (Malvern). The measurements were taken at optical density higher than 25% and the measurement was set for spherical particles with appropriate refractive indices for PLGA and water. We have documented the surface area moment mean diameters (D [3,2]) herein. While the Mastersizer measures many different types of diameters based on different mathematical models, D [3,2] is suitable for this study. It factors in the overall surface area of the particles for computing the diameter, which is the property of interest for adsorption of r-hGH [17]. The average diameters and standard deviations were calculated mathematically for three consecutive batches.

The bulk density (ϱ_b) of the powder was calculated by filling a calibrated 0.5 cc (V_b) syringe with microparticle sample of known mass (M), such that $\varrho_b = M/V_b$.

True density of the MPs was calculated using gas psychometry. The microparticle sample of known mass was added to the measurement cell of the Quant chrome manual micro-pycnometer. The pressure in the cell was brought to 17 psi with the help of the flow valve, and the stabilized pressures with (P1) and without (P2) the sample cell volume accounted for were measured. The average of the P1/P2 ratio was used to compute the true density of the microparticle samples [18].

Using the densities, the final porosity and mass mean aerodynamic diameters were calculated using the equations 3 and 4 [19, 20].

Mean Mass Aerodynamic Diameter (MMAD) = $d_{avg} (\varrho / \varrho_0 X)^{1/2}$ [20] _____Equation 3

Intra-particulate porosity (Ɛ) = (1 – (ϱ/ϱtrue)) x 100 [19] _____Equation 4

Where davg is the average of diameters measured Mastersizer, ϱ is the density of the microparticle powder, ϱ0 is the reference density of PLGA which is 1.34 g/cc, ϱtrue is the true density measured by helium gas pycnometer, and X is the shape factor, which is 1 for the spherical particles [20].

3.4. Evaluation of PEG multifunctionality:

To characterize PEG mediated plasticization, thermal properties of porous PLGA MPs with and without PEG were measured using Differential Scanning Calorimetry (DSC). Samples of approximately 7mg were weighed and sealed hermetically in an aluminum pan. They were scanned between 10oC to 80oC at 10oC per minute and compared to an empty pan under nitrogen atmosphere.

Zeta potential of MPs with and without PEG was measured using dynamic light scattering with Malvern Instrument's Nano ZS (ZEN3600). Dilute dispersion of MPs was prepared by adding MPs to the 1 ml Eppendorf centrifuge tube containing purified water, gently stirred for ~2 s on a vortex stirrer (Vortex genie, K-550-G, Scientific-Industries, Inc.). Zeta potential measurements were done separately in a folded capillary cell (DTS1060) designed especially for zeta potential measurements.

4. Results and Discussion

4.1. Spray drying:

Spray drying produced a free flowing, dry powder which was collected for further studies. Pore former leaching was verified by mass loss of the particles before and after the water treatment, filtration and lyophilization. Figure 1 shows the schematic working of the spray dryer.

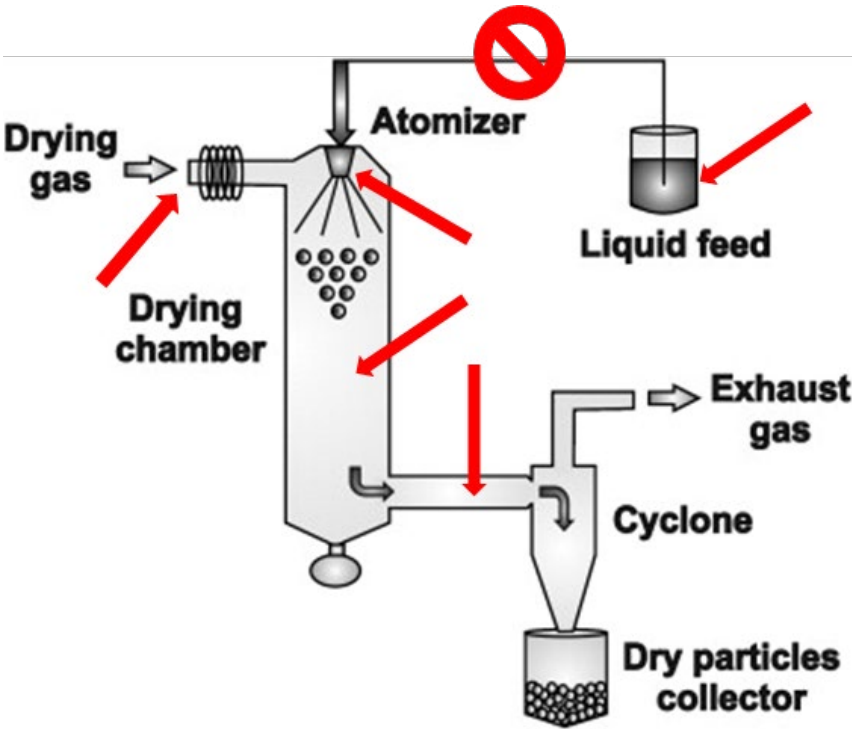

Figure 1: Troubleshooting the spray drying process for identification of the sources of error.

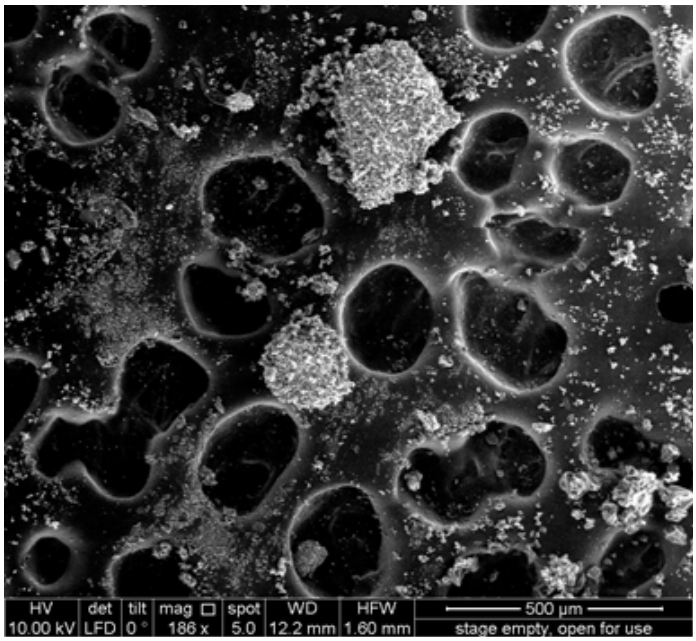

Figure 2: SEM micrograph showing the morphology of films formed within the collection chamber

In the preliminary experiments, we observed formation of sticky films within the collection chamber. The SEM micrograph showing the morphology of a film sample is shown in figure 2. Observation of this film like substance was attributed to improper drying of porous MPs. We believed that changing the process parameters – increasing the temperature and air flow rate, decreasing the feed concentration and flow rate, or altering the geometries of the nozzle and collection chamber – should help mitigate this issue (figure 1). However, the film-formation was later attributed to the incompatibility of the feed tubing with dichloromethane, and using tetrahydrofuran helped obtain particles.

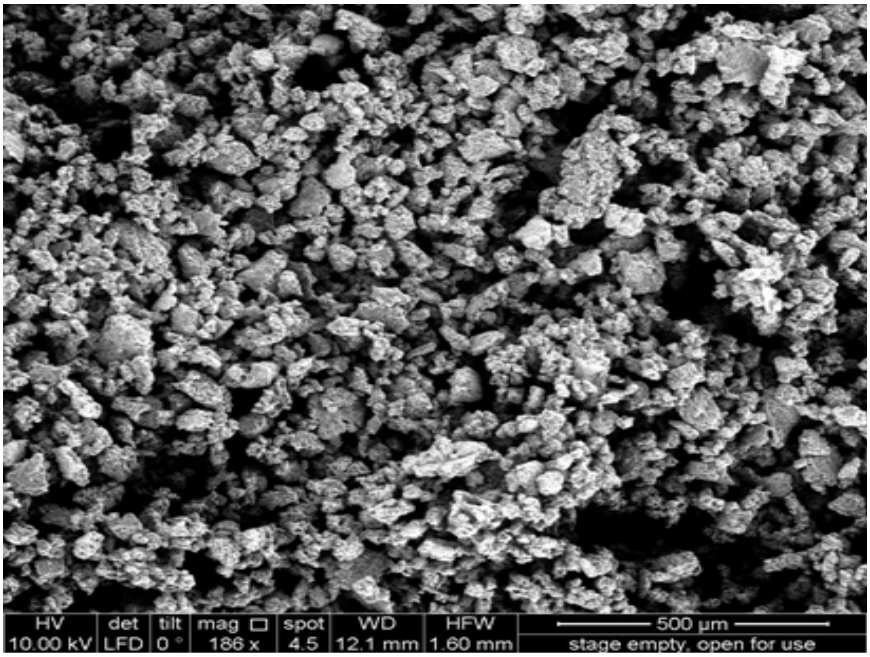

Figure 3: SEM micrograph showing the morphology of cloud shaped MPs.

The particles thus obtained were cloud shaped and aggregated (figure 3). Drying of MPs in a spray dryer is a complex thermodynamic process – and excess drying temperature can lead to flash evaporation of the solvent from the core of the MPs, thereby tearing the particles open. Spherical particles were obtained when the operation temperature was reduced (figure 4).

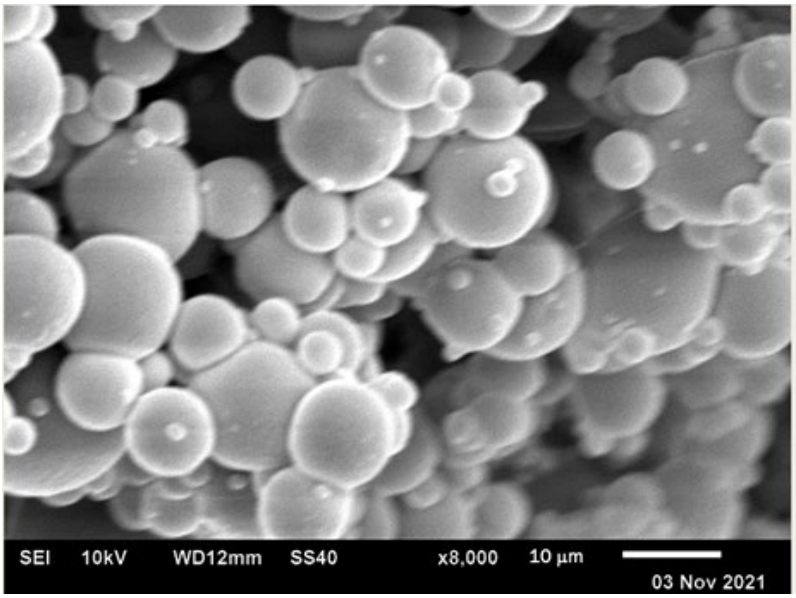

Figure 4. SEM micrographs showing the morphology of spherical MPs because of temperature control.

4.2. Optimization of spray drying process parameters using DOE

4.2.1. Design of experiments (Box-Behnken design):

The experimental runs designed by Design Expert ® were conducted in the random sequence designed by the software, to evaluate the influence of the process parameters on the quality and quantity of the final product (table 1). Maximum yield of MPs, with diameters ranging from 5µm to 12µm, were the key objectives behind implementation of RSM. Three levels were selected for each independent variable to perceive a presence of any interactions between them. RSM was employed successfully for optimization of spray drying process parameters.

Box Behnken design was used for optimization. As figure 5 represents, this design involves working in a cubicle three-dimensional state of parameters to determine a point within this cube where the response is the most favorable. Each point in the cube is a unique combination of the three process parameters. By performing a limited set of randomized trials, the software predicts the value of equations for each combination of process parameters – that is, each point within the cube.

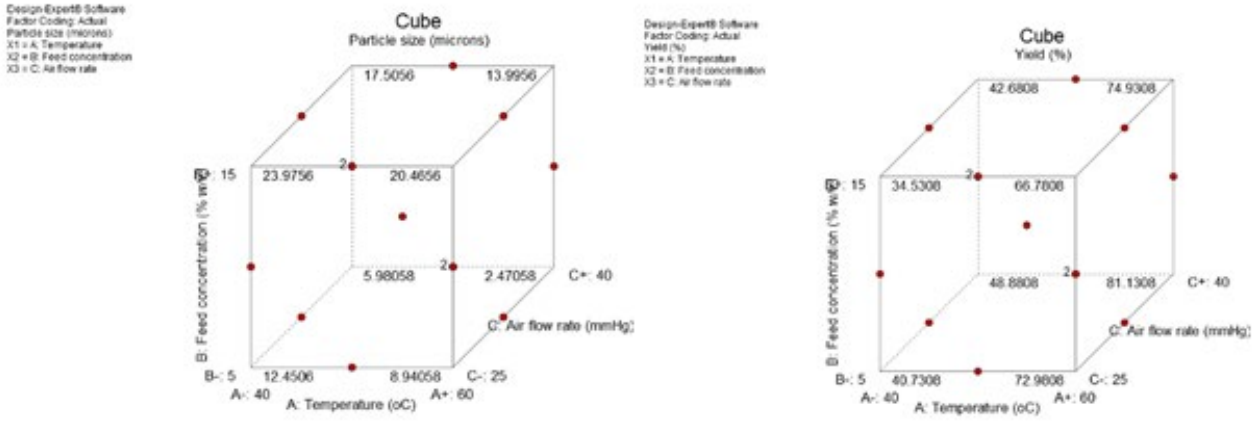

Figure 5: Design space obtained using the Box-Behnken design – variation in responses with changing factor levels along the edges and center points of a cube.

4.2.2. Model fitting and analysis of variance (ANOVA):

Results obtained from randomized experiments were analyzed in the software to confirm their statistical significance. In case of model fitting, both responses fit in a linear pattern. It was found that the linear model was statistically significant. P values (probability) of less than 0.05 indicated the significance of the response surface linear model, as depicted in ANOVA. Furthermore, the correlation coefficients for regression (R2) were found to be 0.77 (predicted 0.63) and 0.96 (predicted 0.94) for particle size and percentage yield respectively. Difference of less than 0.2 between the experimental and predicted R2 values is an indicator of model robustness. A_{deq} precision is the measure of signal to noise ratio and was found to be 11.13 for particle size and 26.24 for yield. Typically, A_{deq} value higher than 4 is desirable for an ideal model. Data generated by implementing the design showed good model fitting and was used for construction of the design space.

Effect of variables on responses was stated using polynomial equations, wherein the impacts of individual factors and their interactions are studied using ANOVA. The final mathematical models, in terms of coded factors, for both the response variables are stated in equations 5 and 6 respectively.

Particle Size (µm) = 24.4914 – 0.1755 * Temperature (oC) + 1.1525 * Feed concentration (%w/v) – 0.4313 * Air Flow Rate (mmHg) ……. Equation 5

% Yield (%) = -34.2526 + 1.6125 * Temperature (oC) – 0.6200 * Feed concentration (%w/v) + 0.5433 * Air Flow Rate (mmHg) ……. Equation 6

The equations represent the coefficient of intercept and first order main effects. Absence of higher order terms denotes the absence of interactions between factors and synergistic effect in favor of a response. Negative signs indicate the adverse effect of the factor on the response.

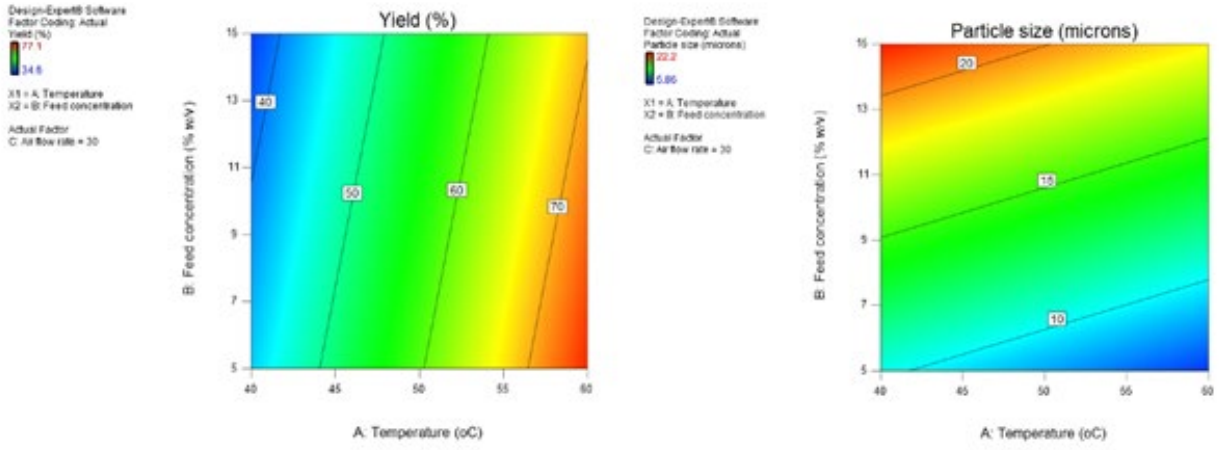

Figure 6: Contour plots for the optimization of particle size and % yield as a function of Temperature and Feed Concentration at constant Air Flow Rate.

Mathematical data generated using multiple linear regression analysis was employed to generate contour plots (figure 6) and 3D response surfaces (figure 7). 3D response surface graphs are plotted by varying two factors while keeping one factor constant. At a constant air flow rate, higher particle size seems to be favored by higher feed concentration and lower temperatures. Opposite trend is observed for yield, increasing the temperature, and decreasing the feed concentration at constant air flow rate seems to be favoring the yield.

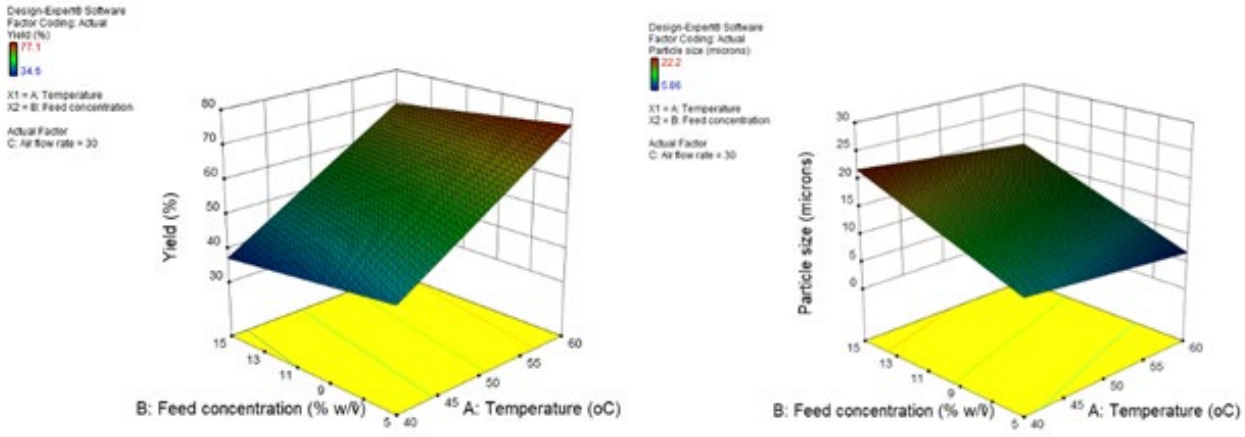

Figure 7. Response surfaces for the optimization of particle size and % yield as a function of Temperature and Feed Concentration at constant Air Flow Rate.

4.2.3. Model validation

Validation of the response surface model was carried out by comparing the experimental results with the predicted responses generated by the Stat-Ease software (Table 2). The target allotted was maximum percentage yield, while maintaining the particle size between 5µm to 12µm. Based on this, the software predicted values, also known as 'points', for the independent variables. Points were selected to assure experimental reproducibility by considering desirability factor close to one. 2 µm (+/-) deviations from particle size and 5% deviation from the yield were permitted during validation. Point confirmation showed that the predicted and experimental values were in close compliance for both responses (table 2). Apart from response confirmation, ANOVA and regression equations strengthened the reliability of the model.

Parameter	Predicted	Actual
Temperature (oC)	59.8892	60
Feed concentration (%w/v)	10.8215	11
Air flow rate (mmHg)	39.799	40
Yield	77.2337	70.78 (4.39)
Particle size	9.28594	9.37 (1.81)

Table 2. DoE model validation by point prediction and evaluation of responses

	Blank PLGA MPs	PLGA/PEG MPs
Glass Transition Temperature (oC)	40.47	36.72
Properties	Amorphous	Amorphous
Zeta Potential (mV)	-41.1	-68.1

Table 3. Evaluation of PLGA plasticization effects of PEG.

4.3. Microparticle Characterization

The average diameters of the porous MPs measured by laser diffraction were in the range of 5 to 23µm. We observed that the percentage yield varied between 30% and 80% for our experiments. The mass mean aerodynamic diameter was calculated theoretically using equation 3 (Table 1). The MPs were found to have aerodynamic diameters of 3 to 10µm (Table 1). The bulk densities of the MPs were between 0.1 g/cc to 0.4 g/cc (Table 1).

Biodegradable, polymeric microcarriers have been an attractive platform for sustained delivery of therapeutics to the lungs, owing to their ability to achieve tailored release, retention and deposition in the pulmonary cavity and non-invasive nature.

Human lungs, however, have an efficient clearance mechanism of 'mucociliary escalator' system and pulmonary macrophages, that effectively remove foreign particulate matter from the lungs, including the therapeutics, before they reach the target site [21-23]. To evade these routes of clearance, it has been established that large, porous MPs with densities less than 0.4 g/cm^3, diameters greater than 5µm and aerodynamic diameters below 6µm [1] can circumvent the phagocytic clearance and mucociliary clearance. In addition, owing to their low densities, they can be aerosolized more effectively from a dry powder inhalation (DPI) formulation, thereby achieving higher respirable fractions of inhaled therapeutics. Moreover, particles smaller than 5µm tend to agglomerate due to van der Waals and electrostatic forces [02].

Variations in particle size were a function of process parameters. The concentration of feed is a main driver of the globule size of the atomized liquid feed. As the feed concentration increases, the viscosity increases. This implies a higher force is required to atomize the feed. Therefore, we observed a direct proportionality between the feed concentration and the particle size. Evaporation of liquid from a droplet to yield a particle is a complex heat and mass transfer process – which begins by evaporation of liquid from the outermost surface. As the process progresses, the liquid in the interior diffuses to the surface and evaporates. At higher feed concentration, the viscosity of the liquid inside the external dried particle core is higher, which therefore slows down the diffusion. This might imply that at higher feed concentrations, the particles may not have completely dried – which is another explanation for the larger particle size. The globule size of the atomized liquid decreases as the atomizing air pressure increases. Smaller globules, in turn, produce smaller MPs. Decrease in particle size with increasing atomizing air pressure has also been corroborated. Equation 5 also shows an inverse proportionality between temperature and globule size. This may seem a bit counter-intuitive at first. However, when the inlet air temperature is higher, the outer surface hardens quickly, thereby preventing the solvent inside to escape. It has also been established, that a certain thickness of the outer dried layer is required to impart a mechanical intactness of the particle [24, 25].

A higher yield was characteristic of excellent flow properties of porous MPs, while lower yield was accompanied by sticking and aggregation. As the feed concentration increases, the solution viscosity increases, and bigger globules are formed. These globules are relatively difficult to dry and may therefore form aggregates or stick to the walls of the spray drying equipment. Incomplete drying of microparticle cores may lead to eventual aggregation and lack of storage stability. Increase in temperature and atomizing air flow rate aid in quicker drying and smaller droplets, which in turn are more pliable to collection.

The true density, measured by helium psychometry, is a measure of the 'real' volume of the sample, which is the total material volume available for gas adsorption. We observed that the real volume, and therefore the true density was conserved at all processing parameters. The overall porosity of the MPs, which is a function of the true volume (equation 4), is also conserved for all processing parameters.

References

1. Kwon, M. J., Bae, J. H., Kim, J. J., Na, K., Lee, E. S. (2007). Long acting porous microparticle for pulmonary protein delivery. International journal of pharmaceutics, 333(1-2), 5-9.
2. Yang, Y., Bajaj, N., Xu, P., Ohn, K., Tsifansky, M. D., et al. (2009). Development of highly porous large PLGA microparticles for pulmonary drug delivery. Biomaterials, 30(10), 1947-1953.
3. Arpagaus, C. (2019). PLA/PLGA nanoparticles prepared by nano spray drying. Journal of Pharmaceutical Investigation, 49, 405-426.
4. Schafroth, N., Arpagaus, C., Jadhav, U. Y., Makne, S., Douroumis, D. (2012). Nano and microparticle engineering of water insoluble drugs using a novel spray-drying process. Colloids and surfaces B: Biointerfaces, 90, 8-15.
5. Mok, H., Park, T. G. (2008). Water-free microencapsulation of proteins within PLGA microparticles by spray drying using PEG-assisted protein solubilization technique in organic solvent. European Journal of Pharmaceutics and Biopharmaceutics, 70(1), 137-144.
6. Straub, J. A., Chickering, D. E., Church, C. C., Shah, B., Hanlon, T., et al. (2005). Porous PLGA microparticles: AI-700, an intravenously administered ultrasound contrast agent for use in echocardiography. Journal of controlled release, 108(1), 21-32.
7. Ahmed, A. R., Bodmeier, R. (2009). Preparation of preformed porous PLGA microparticles and antisense oligonucleotides loading. European journal of pharmaceutics and biopharmaceutics, 71(2), 264-270.
8. Nishimura, S., Takami, T., Murakami, Y. (2017). Porous PLGA microparticles formed by "one-step" emulsification for pulmonary drug delivery: The surface morphology and the aerodynamic properties. Colloids and Surfaces B: Biointerfaces, 159, 318-326.
9. Freitas, S., Merkle, H. P., Gander, B. (2004). Ultrasonic atomisation into reduced pressure atmosphere—envisaging aseptic spray-drying for microencapsulation. Journal of controlled Release, 95(2), 185-195.
10. Tan, L. P., Venkatraman, S. S., Sung, P. F., Wang, X. T. (2004). Effect of plasticization on heparin release from biodegradable matrices. International journal of pharmaceutics, 283(1-2), 89-96.
11. Mi, F. L., Shyu, S. S., Lin, Y. M., Wu, Y. B., Peng, C. K., et al. (2003). Chitin/PLGA blend microspheres as a biodegradable drug delivery system: a new delivery system for protein. Biomaterials, 24(27), 5023-5036.
12. Schloegl, W., Marschall, V., Witting, M. Y., Volkmer, E., Drosse, I., et al. (2012). Porosity and mechanically optimized PLGA based in situ hardening systems. European journal of pharmaceutics and biopharmaceutics, 82(3), 554-562.
13. Gosau, M., Müller, B. W. (2010). Release of gentamicin sulphate from biodegradable PLGA-implants produced by hot melt extrusion. Die Pharmazie-An International Journal of Pharmaceutical Sciences, 65(7), 487-492.

14. Jain, R. A., Rhodes, C. T., Railkar, A. M., Malick, A. W., Shah, N. H. (2000). Controlled release of drugs from injectable in situ formed biodegradable PLGA microspheres: effect of various formulation variables. European journal of pharmaceutics and biopharmaceutics, 50(2), 257-262.
15. Rose, S. R. (2019). Management options for pediatric growth hormone deficiency. Expert Opinion on Orphan Drugs, 7(2), 47-55.
16. Shah, V. R., Gupta, P. K. (2018). Structural stability of recombinant human growth hormone (r-hgh) as a function of polymer surface properties. Pharmaceutical research, 35, 1-18.
17. Sodha, S., Gupta, P. (2023). PLGA and PEG based porous microparticles as vehicles for pulmonary Somatropin delivery. European Journal of Pharmaceutics and Biopharmaceutics.
18. ISIS Pycnometry, (n.d.). (accessed August 9, 2021).
19. Nasr, M., Awad, G. A., Mansour, S., Al Shamy, A., Mortada, N. D. (2013). Hydrophilic versus hydrophobic porogens for engineering of poly (lactide-co-glycolide) microparticles containing risedronate sodium. Pharmaceutical Development and Technology, 18(5), 1078-1088.
20. Arnold, M. M., Gorman, E. M., Schieber, L. J., Munson, E. J., Berkland, C. (2007). NanoCipro encapsulation in monodisperse large porous PLGA microparticles. Journal of Controlled Release, 121(1-2), 100-109.
21. Pakulska, M. M., Elliott Donaghue, I., Obermeyer, J. M., Tuladhar, A., McLaughlin, C. K., et al. (2016). Encapsulation-free controlled release: Electrostatic adsorption eliminates the need for protein encapsulation in PLGA nanoparticles. Science advances, 2(5), e1600519.
22. Lakowicz, J. R. (Ed.). (2006). Principles of fluorescence spectroscopy. Boston, MA: springer US.
23. Edwards, D. A., Hanes, J., Caponetti, G., Hrkach, J., Ben-Jebria, A. (1997). Large porous particles for pulmonary drug delivery. Science, 276(5320), 1868-1872.
24. Elversson, J., Millqvist-Fureby, A. (2005). Particle size and density in spray drying—effects of carbohydrate properties. Journal of pharmaceutical sciences, 94(9), 2049-2060.
25. Vehring, R. (2008). Pharmaceutical particle engineering via spray drying. Pharmaceutical research, 25, 999-1022.